**Atmospheric
Measurement
Techniques
Discussions**

NO$_2$ observations over the western Pacific and Indian Ocean by MAX-DOAS on *Kaiyo*, a Japanese research vessel

H. Takashima[1], H. Irie[1], Y. Kanaya[1], and F. Syamsudin[2]

[1]Research Institute for Global Change (RIGC), Japan Agency for Marine-Earth Science and Technology (JAMSTEC), 3173-25 Showa-machi, Kanazawa-ku, Yokohama, Kanagawa 236-0001, Japan
[2]Agency for the Assessment and Application of Technology (BPPT), BPPT New Bldg 19th Fl., Jalan M.H. Thamrin 8, Jakarta 10340, Indonesia

Correspondence to: H. Takashima (hisahiro@jamstec.go.jp)

Discussion Paper | Discussion Paper | Discussion Paper | Discussion Paper

AMTD

4, 6069–6095, 2011

NO$_2$ observations over the western Pacific and Indian Ocean

H. Takashima et al.

Title Page	
Abstract	Introduction
Conclusions	References
Tables	Figures

◄◄	►►
◄	►
Back	Close

Full Screen / Esc

Printer-friendly Version

Interactive Discussion

Abstract

Nitrogen dioxide (NO_2) profile retrievals were performed by ship-borne Multi-Axis Differential Optical Absorption Spectroscopy (MAX-DOAS) using a compact/low-power spectrometer on the Japanese research vessel *Kaiyo* during two ocean cruises around

5 Japan and Japan-Bali (Indonesia)-Indian Ocean. DOAS analysis using a 425–450 nm fitting window revealed a clear land–ocean contrast in NO_2 differential slant column densities (DSCDs) but poor fitting results and negative values, especially at low elevation angles at low latitudes ($<\sim20°$ N). The poor fitting resulted in sparse NO_2 volume mixing ratio (VMR) data for the 0–1 km layer after applying our vertical profile retrieval

10 method. In contrast, NO_2 VMRs retrieved using fitting results from 460–490 nm are positive even at low latitudes, while they are reasonably similar to those obtained from 425–450 nm at mid-latitudes. Because NO_2 DSCD for 425–450 nm shows a negative correlation with water vapor (H_2O) DSCD, the poor fitting appears to be due primarily to interference by H_2O. We analyzed a 338–370 nm fitting window, which is free from

15 H_2O, and found good agreement between NO_2 VMRs retrieved from 460–490 nm and 338–370 nm, even at low latitudes, at NO_2 VMRs higher than ~0.2 ppbv. The results indicate that the background value of NO_2 VMR over the western Pacific and Indian Ocean during the cruises was less than ~0.2 ppbv, with occasional enhancement to levels of ~0.2–0.4 ppbv.

1 Introduction

20 Multi-Axis Differential Optical Absorption Spectroscopy (MAX-DOAS) is a recently developed remote sensing technique designed for atmospheric aerosol and gas profile measurements using scattered solar radiation at several elevation angles (e.g. Hönninger et al., 2004; Wagner et al., 2004; Sinreich et al., 2005; Frieß et al., 2006). It

25 is useful for measuring a priori profiles for satellite retrievals and for validating chemical transport models.

Recently, multi-platform measurements by MAX-DOAS, such as from aircraft (e.g. Volkamer et al., 2009) and ocean vessels (e.g. Wagner et al., 2007; Volkamer et al.,

Title Page

Abstract | Introduction

Conclusions | References

Tables | Figures

|◄ | ►|

◄ | ►

Back | Close

Full Screen / Esc

Printer-friendly Version

Interactive Discussion

2009; Sinreich et al., 2010), have been developed. Ship-borne measurements provide information on background concentrations over the ocean and can be used to clarify transport processes from polluted areas to the ocean, emissions from ocean to air, and emissions from ships. However, even in the case of NO_2, spatial and temporal varia-
5 tions over the ocean are not fully understood, due in part to the difficulties encountered in measuring low concentrations.

In general, MAX-DOAS measures the trace gas content over a long light path (up to $\sim$10 km) with low elevation angles, thereby enabling the detection of low concentrations of the components of interest or weak absorbers near the ground. Thus, MAX-DOAS is
10 useful for quantifying tropospheric trace gas over remote areas/ocean, where concentrations of the component of interest are generally low. As an example, NO_2 measurements by MAX-DOAS have been conducted at a remote Japanese island, Okinawa Island, yielding concentrations as low as $\sim$0.2 ppbv (Takashima et al., 2011).

Since 2007, the Japan Agency for Marine-Earth Science and Technology/Research
15 Institute for Global Change (JAMSTEC/RIGC) has been conducting continuous MAX-DOAS measurements at several sites in Asia and Russia using compact, low-power spectrometers (e.g. Irie et al., 2009, 2011; Takashima et al., 2009, 2011). The instrument has been validated with other instruments, yielding differences of less than $\sim$10 % for NO_2 and oxygen dimer (O_4) differential slant column densities (DSCDs) (Roscoe et
20 al., 2010). Here, we report on the development of a MAX-DOAS instrument for use on ocean vessels, using an active-type gimbal to keep the telescope horizontal.

As a first step, we focus only on NO_2 because it is somewhat easier to retrieve than other components, although MAX-DOAS has the potential to perform simultaneous profile measurements on aerosol and several gas components, such as NO_2, water
25 vapor (H_2O), SO_2, IO, BrO, HCHO, and CHOCHO (e.g. Irie et al., 2011). We also performed a sensitivity analysis with three fitting windows for NO_2 retrieval and we discuss the detection limit of the NO_2 retrievals, because the sensitivity has yet to be fully investigated.

2   Measurements

2.1   Two ocean cruises on the Japanese R/V *K*aiyo

Aerosol and gas measurements by MAX-DOAS were continuously conducted during two ocean cruises on the Japanese R/V *Kaiyo* of JAMSTEC. The first cruise (KY08-05) was undertaken during 10–17 July 2008 from Yura (Wakayama Prefecture; 135.11° E, 33.96° N) to Yokosuka (Kanagawa Prefecture; 139.68° E, 35.28° N) in Japan (Fig. 1). The second cruise (KY09-01) was conducted from 5 February to 10 May 2009 from Yokohama (Japan; 139.65° E, 35.45° N) to Bari (Indonesia; 115.21° E, 8.74° S), the Indian Ocean, Bari again, and finally returning to Yokohama (Fig. 1). We did not perform measurements in the territorial waters of Guam (United States) during cruise KY09-01 because we did not obtain permission from the relevant authorities. Note that this study is the first to report MAX-DOAS measurements over the western Pacific and Indian Ocean.

2.2   Compact, low-power instruments for MAX-DOAS

A compact, low-power and low-cost instrument for MAX-DOAS has been developed by JAMSTEC/RIGC and PREDE Co., Ltd. (Tokyo, Japan), and the instrument has been used for continuous measurements at several sites in Asia and Russia. In this study, we developed the instrument for use on ocean vessels by employing an active-type gimbal to keep the telescope horizontal on the vessel. The gimbal-mounted telescope unit was installed on the top deck of the vessel and the line of sight was toward the starboard side (Fig. 2). The movable mirror of the telescope unit rotates through six different elevation angles (ELs) of 3°, 5°, 10°, 20°, 30°, and 70° every 30 min, with a field of view of ~0.9°.

For the first cruise (KY08-05), a miniaturized UV/visible spectrometer (USB4000, Ocean Optics) was installed inside the telescope unit, and the spectra data were recorded by a laptop located indoors on the vessel. The telescope and spectrometer

Title Page

Abstract | Introduction

Conclusions | References

Tables | Figures

◄ | ►

◄ | ►

Back | Close

Full Screen / Esc

Printer-friendly Version

Interactive Discussion

H. Takashima et al.

were connected to each other by a 1-m (KY08-05) or 10-m (the second cruise, KY09-01) fiber optic bundle cable that consists of seven cores with radii of 100 μm. The typical exposure time was 0.08 s, and the spectra data were averaged and recorded every second by a laptop located indoors. Measurements were made over the spectral range of 230 to 560 nm with a spectral resolution of ∼0.6–0.7 nm. To suppress background noise and wavelength shifts of the spectrum, the temperature of the spectrometer was kept at 45 °C for KY08-05 and at 40 °C for KY09-01, for the entire observation period. For KY09-01, the spectrometer (USB4000) was installed indoors, aiming at better temperature control.

For comparison with in situ measurements, we use MAX-DOAS data obtained at Yokosuka, Japan (35.32° N, 139.65° E), which have been measured continuously since April 2007 using basically the same instrument as that used at Okinawa (Takashima et al., 2009), employing a USB4000 spectrometer and 5-m fiber optics. The azimuth angle of the observations was set to +37.0 from north (the plus sign indicates a clockwise direction). A movable mirror turns through six different ELs (3°, 5°, 10°, 20°, 30°, and 90°) every 30 min, with a field of view of <1°. The spectrometer was kept 20 °C.

2.3 Active gimbal system

To keep the telescope unit horizontal on the vessel, it was mounted on an active-gimbal developed by JAMSTEC/RIGC and PREDE. In this system, the gimbal is controlled horizontally by reducing the difference between the standard horizontal level and the present level for both the roll and pitch angles, using two inclinometers (SEIKA Mikrosystemtechnik GmbH, N2).

To monitor how well the gimbal maintains a horizontal orientation, we installed another sensor inside the telescope unit (Honeywell, HMR3500) and recorded the roll and pitch angels at a repetition rate of 5 Hz. For the spectral analysis, spectra data were selected with a criterion for the elevation angle to be within ±0.2° of the target (see below). In addition, we recorded the heading of the vessel, the roll and pitch angles of the vessel, longitude, latitude, and time.

Figure 3 shows an example of the pitch and roll angles of the vessel and the tele-
scope unit. The telescope unit was installed on the starboard-side (roll) direction of
the viewing azimuth angle. The figure shows that the orientation of the telescope unit
was generally controlled well even when the roll and pitch angles of the vessel reached
>2 degrees. During the KY08-05 and KY09-01 cruises, the telescope was kept within
$\pm 0.2°$ of the target elevation angle for ~60 % of the time. In general, in the case of a
regular cycle of ship motion (e.g. a sine function), the gimbal performs well in control-
ling the horizontal level, but it is commonly unable to control the horizontal level in the
case of an irregular cycle. Figure 3 shows an example of variation of the maximum
intensity of the spectrum, in which we can see change in the intensity corresponding
to change in the elevation angle (from 3° to 5°).

3 Data analysis

The measured 1-s spectra were selected with a criterion for the elevation angle to be
within $\pm 0.2°$ of the target elevation angle and averaged every 1 min. Here, we excluded
spectra data for periods when we changed the target elevation angle of the telescope-
unit mirror. The azimuth of the heading of the vessel, longitude, altitude were also
averaged every 1 min.

To retrieve a vertical profile of NO_2 concentration, we used the Japanese MAX-DOAS
profile retrieval algorithm, version 1 (JM1) (Irie et al., 2011). The averaged spectrum
was analyzed using the DOAS method (Platt, 1994), employing nonlinear least squares
spectral fitting (Rodgers, 2000) to derive the DSCD of the oxygen collision complex
(O_2-O_2 or O_4) and NO_2. Here, DSCD is defined as the difference between the column
concentration integrated along the sunlight path measured at a low EL (EL < 70° to
derive the DSCD of the oxygen collision complex) and that at EL = 70° to derive the
DSCD of the oxygen collision complex.

The box air mass factor (A_{box}), which is defined as the air mass factor for a given
layer, was derived from the O_4 DSCD inversion with the Monte Carlo Atmospheric Ra-
diative Transfer Simulator (MCARaTS) (Iwabuchi, 2006). Using the A_{box}, we retrieved

NO$_2$ profiles in the lower troposphere with a vertical step of 1 km from the NO$_2$ DSCD measurements. Details of the retrieval algorithm have been described elsewhere (e.g. Irie et al., 2008, 2011; Takashima et al., 2011).

We used NO$_2$ absorption cross-section data at 294 K of Vandaele et al. (1998), O$_4$ data of Hermans et al. (http://spectrolab.aeronomie.be/o2.htm), H$_2$O data of the year 2004 edition of the High-Resolution Transmission (HITRAN) database (fitting windows and absorbers fitted in DOAS analysis are shown in Table 1). In the retrieval, we applied the 460–490 nm standard fitting window of JM1, but we also used the 425–450 nm window, which is one of the most widely used for NO$_2$ retrieval (e.g. Boersma et al., 2004). We also performed an additional sensitivity analysis using a fitting window of 338–370 nm, and using different NO$_2$ cross-section data at 220 K (Vandaele et al., 1998).

4   Results and discussion

4.1   NO$_2$ retrieval for three fitting windows

First, the NO$_2$ profile was retrieved using the JM1 algorithm with a standard fitting window of 460–490 nm. Figure 4 shows NO$_2$ concentrations for the 0–1 km layer, close to mainland Japan (the area with highest concentrations during the cruises). A clear land-ocean contrast is observed: during KY08-05, NO$_2$ concentrations were low over the ocean (<1 ppbv), with no clear diurnal variations; in contrast, concentrations were high (>1 ppbv) and with a clear diurnal variation near the coast or when in port (19–21 July 2009, Fig. 4a). Although the location of the port at the end of the KY08-05 cruise was located ∼5 km from the Yokosuka site, there is generally good agreement between the two datasets, with similar diurnal maxima (in the morning/evening) and minima (∼1–2 ppbv around noon). For the KY09-01 cruise, the port (the vessel) was located ∼14 km from the Yokosuka site (e.g. 5–8 February), but similar diurnal variations were also observed. These findings indicate successful NO$_2$ measurements from onboard the vessel, at least for the high concentrations observed near Japan/mid-latitudes.

NO$_2$ observations over the western Pacific and Indian Ocean

H. Takashima et al.

DOAS analysis using a 425–450 nm fitting window also revealed a clear land-ocean contrast in NO$_2$ DSCDs, with quite good agreement over the Japan region (Fig. 5a, c), but poor fitting results (Fig. 6c) and negative DSCD values, especially at low elevation angles at low latitudes (in the cause of Fig. 6c, the NO$_2$ DSCD was positive). In general,

5   lower NO$_2$ DSCD was obtained at lower ELs (see the following paragraph and Fig. 7). This resulted in sparse NO$_2$ volume mixing ratio (VMR) data after applying our vertical profile retrieval methods (Fig. 5).

To consider the effect of H$_2$O in the fitting for the 425–450 nm window, the relationship between H$_2$O DSCD and NO$_2$ DSCD was investigated (Fig. 7); there is a clear negative

10   correlation between the two. At the same time the fitting residual is high for high H$_2$O DSCD (not shown). These results suggest that the poor fitting at 425–450 nm is due in part to the H$_2$O interference in the fitting. At lower elevation angles, the amount of H$_2$O is generally high; thus, the fitting is generally poor. It should be noted that the H$_2$O DSCD for 425–450 nm is consistent with that for 460–690 nm (figure not shown; a

15   correlation coefficient (r) for EL = 3° was 0.98). We also investigated other relationships and found a negative correlation between H$_2$O DSCD and the Ring effect (not shown), suggesting that the Ring effect also contributed to the poor fitting (Fig. 6c).

We next employed an ultraviolet (UV) fitting window (338–370 nm), which is completely free from absorption by H$_2$O. Here, we considered O$_4$ for 338–370 nm to derive

20   NO$_2$ VMR. Although the retrieval errors were higher than in the case of 460–490 nm (Table 2; see Sect. 4.2) due in part to the lower intensity (particularly in the morning/evening), there is generally good agreement between NO$_2$ (460–490 nm) and NO$_2$ (338–370 nm) concentrations for concentrations higher than ∼0.2 ppbv (Fig. 8). This result suggests that our MAX-DOAS can at least detect NO$_2$ concentrations as low as

25   ∼0.2 ppbv for the 0–1 km layer. The results also indicate that the background level over the western Pacific and Indian Ocean during the cruise was less than ∼0.2 ppbv for the 0–1 km layer. The 460–490 nm standard fitting window of JM1 seems to be particularly useful for the retrieval of low NO$_2$ concentrations over the ocean and in H$_2$O-rich areas.

4.2 Sensitivity analysis and error estimates

We next conducted a DOAS analysis using the NO_2 cross-section of 220 K as a sensitivity test of cross-section temperature dependence, revealing a strong correlation between NO_2 concentration using 220 and 294 K cross-sections ($R = 0.99$) but NO_2
5   concentration for 220 K systematically underestimates NO_2 for 294 K of ∼30 % (Fig. 9). Because the actual temperature at 0–1 km is unlikely to have been as cold as 220 K, the sensitivity to the actual temperature variation would have been much smaller than that obtained from the DOAS analysis. Sanders (1996) and more recently Boersma et al. (2004) reported the temperature dependence of trace gas in tropospheric NO_2
10 retrieval. Subsequently, A. Richter et al. (personal communication, 2011) indicated that the retrieved NO_2 concentration using a 425–450 nm window shows a linear increase with applying a warmer cross-section, because the NO_2 cross-section at high temperatures is smaller than that at low temperatures. In their analysis, the temperature dependence is ∼0.36 % K^{-1} for the 425–450 nm fitting window, which is similar to our
15 result of ∼30 % $(294–220\,K)^{-1} = 0.4\,\%\,K^{-1}$, despite the different fitting window used in the two studies.

Random and systematic errors for each MAX-DOAS measurement were estimated following Irie et al. (2011) and Takashima et al. (2011). The random error was estimated from the residual in the fitting of the NO_2 DSCD, and the systematic error was estimated
20 assuming an additional 30 % change in aerosol optical depth (AOD), for which A_{box} varies accordingly.

The estimated random and systematic errors in the NO_2 concentration for the 460–490 nm standard window during the KY09-01 cruise over the ocean were 0.009 ppbv (7.6 %) and 0.015 ppbv (12.6 %), respectively (Table 2). The total error was as small
25 as ∼15 % (∼0.18 ppbv), even in the case of low background values over the remote ocean. These errors were of a similar order to those for the retrieval with the 220 K NO_2 cross-section. Note that the coldest and warmest temperatures below 1 km during KY09-01 were about −20 K (with respect to 294 K) near Japan in February and +3 K

Title Page

Abstract | Introduction

Conclusions | References

Tables | Figures

|◄ | ►|

◄ | ►

Back | Close

Full Screen / Esc

Printer-friendly Version

Interactive Discussion

in the tropics. These correspond to systematic errors of −8 % and +1 %, respectively, based on the derived cross-section temperature dependence of $0.4\,\%\,K^{-1}$. The range of this systematic error ($\sim$9 % for 23 K) is of a smaller order than the total error.

For UV, the errors were higher than those for 460–490 nm, due in part to lower intensity in our observation system, particularly in the morning/evening. The errors obtained near land (in the Japan region) for 460–490 nm are similar to those for 425–450 nm.

The errors over the ocean during KY09-01 are largely consistent with those reported previously for a remote island (Okinawa Island, Japan; for which the systematic and random errors were 12.8 % and 13.0 %, respectively) by Takashima et al. (2011), although these error values (i.e. of the present and previous studies) are much smaller than the background value over the ocean ($<\sim$0.2 ppbv). Note that over the remote ocean, variability in NO_2 concentrations was less than $\sim$0.1 ppbv at 0–1 km, as assessed from a time series (not shown) and from Fig. 10. Therefore, this level ($\sim$0.1 ppbv) may be close to the detection limit of NO_2 concentrations over the remote ocean.

4.3 NO_2 variations over the remote ocean

We next discuss NO_2 variations over the remote ocean retrieved by JM1 with a standard 460–490 nm fitting window for concentrations >0.2 ppbv. Over the remote ocean during cruise KY09-01, NO_2 concentrations were generally very low (<0.5 ppbv at 0–1 km; Fig. 10). The probability density function (PDF) for ≤1 ppbv during KY09-01 (Fig. 11) yields a mode of $\sim 0.1 \pm 0.1$ ppbv, which appears to correspond to the background level over the remote ocean (<0.2 ppbv). This value is similar to those obtained by direct measurements by airplane during the TRACE-P observation campaign, which yielded NO_2 concentrations of less than $\sim$0.05 ppbv over the western Pacific in the marine boundary layer during P3-B Flight 08 (data are available from the NASA TRACE-P Website at http://www-gte.larc.nasa.gov. Figure 11 shows a skewed distribution of NO_2 concentrations with some enhancements, including NO_2 concentrations ($\sim$0.2–0.4 ppbv) higher than the background level, in which the fitting residual for NO_2

Full Screen / Esc

Printer-friendly Version

Interactive Discussion

concentrations of 0.2–0.4 ppbv was as small as ∼8.1×10^{-4} (the median value; an example of the fitting is shown in Fig. 6b).

These enhancements over the remote ocean are also apparent in Fig. 10, with spatial variability. In some cases, the air mass was affected by polluted air (e.g. southwest of Guam, where the air mass was advected from the direction of Guam), but this was infrequently observed. We also tested for the effect of emissions from the research vessel. To avoid such contamination, we analyzed wind data recorded on the vessel and removed potentially contaminated NO_2 data before repeating the analysis; however, no significant difference was observed in the PDF compared with the entire dataset. The enhancement may also reflect emissions from ships over the ocean or long-range rapid transport from polluted areas, as suggested by Takashima et al. (2011). Additional measurements over the ocean are required to quantify the background levels and the nature of spatial-temporal variations over the ocean.

5 Summary

NO_2 measurements by ship-borne MAX-DOAS with a compact/low-power spectrometer were conducted during two ocean cruises, around Japan and Japan-Bali (Indonesia)-Indian Ocean. The telescope was mounted on an active gimbal to ensure it was kept horizontal; it was successfully kept within ±0.2° of the target elevation angle for ∼60 % of the time.

To test the sensitivity of the fitting window for NO_2 retrieval, focusing on low NO_2 concentration over the ocean, we considered windows of 425–450, 460–490, and 338–370 nm. DOAS analysis using a 425–450 nm fitting window, which is widely used for NO_2 retrieval, revealed a clear land-ocean contrast in NO_2 DSCDs but poor fitting results and negative values, especially at low elevation angles at low latitudes. The negative values resulted in sparse NO_2 VMR data, whereas, NO_2 DSCDs retrieved using fitting results from the 460–490 nm standard fitting window of JM1 are positive even at low latitudes, and NO_2 VMRs are very similar to those obtained using a window of

425–450 nm at mid-latitudes. Because the NO_2 DSCD for 425–450 nm has a negative correlation with the H_2O DSCD (Fig. 7), the poor fitting appears to be due to the H_2O interference in the fitting. We analyzed a 338–370 nm fitting window, which is completely free from absorption by H_2O, and found a good agreement between NO_2 VMRs re-
5 trieved from 460–490 nm and 338–370 nm, even at low-latitudes, at NO_2 VMRs higher than ~0.2 ppbv (Fig. 8). Consequently, the 460–490 nm fitting window seems to be useful for the retrieval of low NO_2 concentrations over the ocean.

We also performed a sensitivity analysis using different NO_2 cross-sections (294 K and 220 K) for the 460–490 nm fitting window. The correlation between the two NO_2
10 concentrations was reasonably good, but NO_2 for 220 K systematically underestimates NO_2 for 294 K by ~30 % (Fig. 9).

The results indicate that the background value of NO_2 over the western Pacific and Indian Ocean during the cruises was less than 0.2 ppbv, but occasional enhancement to values of ~0.2–0.4 ppbv was often observed, exceeding the background level. On
15 rare occasions, the air mass was affected by polluted air.

References

Boersma, K. F., Eskes, H. J., and Brinksma, E. J.: Error Analysis for tropospheric NO_2 retrieval
20 from space, J. Geophys. Res. 109, D04311, doi:10.1029/2003JD003962, 2004.
Frieß, U., Monks, P. S., Remedios, J. J., Rozanov, A., Sinreich, R., Wagner, T., and Platt, U.: MAX-DOAS O_4 measurements: a new technique to derive information on atmospheric aerosols: 2. Modeling studies, J. Geophys. Res., 111, D14203, doi:10.1029/2005JD006618, 2006.
25 Hönninger, G., von Friedeburg, C., and Platt, U.: Multi axis differential optical absorption spectroscopy (MAX-DOAS), Atmos. Chem. Phys., 4, 231–254, doi:10.5194/acp-4-231-2004, 2004.
Irie, H., Kanaya, Y., Akimoto, H., Iwabuchi, H., Shimizu, A., and Aoki, K.: First retrieval of tropospheric aerosol profiles using MAX-DOAS and comparison with lidar and sky radiometer
30 measurements, Atmos. Chem. Phys., 8, 341–350, doi:10.5194/acp-8-341-2008, 2008.

Irie, H., Kanaya, Y., Takashima, H., Gleason, J. F., and Wang, Z. F.: Characterization of OMI tropospheric NO_2 measurements in East Asia based on a robust validation comparison, SOLA, 5, 117–120, 2009.

Irie, H., Takashima, H., Kanaya, Y., Boersma, K. F., Gast, L., Wittrock, F., Brunner, D., Zhou, Y., and Van Roozendael, M.: Eight-component retrievals from ground-based MAX-DOAS observations, Atmos. Meas. Tech., 4, 1027–1044, doi:10.5194/amt-4-1027-2011, 2011.

Iwabuchi, H.: Efficient Monte Carlo methods for radiative transfer modeling, J. Atmos. Sci., 63, 2324–2339, 2006.

Platt, U.: Differential optical absorption spectroscopy (DOAS), in: Air Monitoring by Spectroscopic Techniques, 127, John Wiley & Sons, New York, 1994.

Rodgers, C. D.: Inverse methods for atmospheric sounding: Theory and practice, in: Ser. Atmos. Oceanic Planet. Phys., 2, edited by: Taylor, F. W., World Sci., Hackensack, NJ, 2000.

Roscoe, H. K., Van Roozendael, M., Fayt, C., du Piesanie, A., Abuhassan, N., Adams, C., Akrami, M., Cede, A., Chong, J., Clémer, K., Friess, U., Gil Ojeda, M., Goutail, F., Graves, R., Griesfeller, A., Grossmann, K., Hemerijckx, G., Hendrick, F., Herman, J., Hermans, C., Irie, H., Johnston, P. V., Kanaya, Y., Kreher, K., Leigh, R., Merlaud, A., Mount, G. H., Navarro, M., Oetjen, H., Pazmino, A., Perez-Camacho, M., Peters, E., Pinardi, G., Puentedura, O., Richter, A., Schönhardt, A., Shaiganfar, R., Spinei, E., Strong, K., Takashima, H., Vlemmix, T., Vrekoussis, M., Wagner, T., Wittrock, F., Yela, M., Yilmaz, S., Boersma, F., Hains, J., Kroon, M., Piters, A., and Kim, Y. J.: Intercomparison of slant column measurements of NO_2 and O_4 by MAX-DOAS and zenith-sky UV and visible spectrometers, Atmos. Meas. Tech., 3, 1629–1646, doi:10.5194/amt-3-1629-2010, 2010.

Sanders, R. W.: Improved analysis of atmospheric absorption spectra by including the temperature dependence of NO_2, J. Geophys. Res., 101, 20945–20952, doi:10.1029/96JD01699, 1996.

Sinreich, R., Frieß, U., Wagner, T., and Platt, U.: Multi axis differential optical absorption spectroscopy (MAX-DOAS) of gas and aerosol distributions, Faraday Discuss., 130, 153–164, doi:10.1039/B419274P, 2005.

Sinreich, R., Coburn, S., Dix, B., and Volkamer, R.: Ship-based detection of glyoxal over the remote tropical Pacific Ocean, Atmos. Chem. Phys., 10, 11359–11371, doi:10.5194/acp-10-11359-2010, 2010.

Takashima, H., Irie, H., Kanaya, Y., Shimizu, A., Aoki, K., and Akimoto, H.: Atmospheric aerosol variations at Okinawa Island in Japan observed by MAX-DOAS using a new cloud-screening

method, J. Geophys. Res., 114, D18213, doi:10.1029/2009JD011939, 2009.

Takashima, H., Irie, H., Kanaya, Y., and Akimoto, H.: Enhanced NO_2 at Okinawa Island, Japan caused by rapid air mass transport from China as observed by MAX-DOAS, Atmos. Environ., 45, 15, 2593–2597, doi:10.1016/j.atmosenv.2010.10.055, 2011.

Vandaele, A., Hermans, C., Simon, P., Carleer, M., Colin, R., Fally, S., Merienne, M., Jenouvrier, A., and Coquart, B.: Measurements of the NO_2 absorption crosssection from 42,000 cm$_-$1 to 10,000 cm$_-$1 (238e1000 nm) at 220 K and 294 K, J. Quant. Spectrosc. Ra., 59, 171–184, 1998.

Volkamer, R., Coburn, S., Dix, B., and Sinreich, R.: MAX-DOAS observations from ground, ship, and research aircraft: maximizing signal-to-noise to measure 'weak' absorbers, Proc. SPIE 7462, 746203, doi:10.1117/12.826792, 2009.

Wagner, T., Dix, B., von Friedeburg, C., Frieß, U., Sanghavi, S., Sinreich, R., and Platt, U.: MAX-DOAS O_4 measurements, A new technique to derive information on atmospheric aerosols – Principles and information content, J. Geophys. Res., 109, D22205, doi:10.1029/2004JD004904, 2004.

Wagner, T., Ibrahim, O., Sinreich, R., Frieß, U., von Glasow, R., and Platt, U.: Enhanced tropospheric BrO over Antarctic sea ice in mid winter observed by MAX-DOAS on board the research vessel Polarstern, Atmos. Chem. Phys., 7, 3129–3142, doi:10.5194/acp-7-3129-2007, 2007.

Discussion Paper | Discussion Paper | Discussion Paper | Discussion Paper | Discussion Paper |

Title Page

Abstract | Introduction

Conclusions | References

Tables | Figures

◄ | ►

◄ | ►

Back | Close

Full Screen / Esc

Printer-friendly Version

Interactive Discussion

Table 1. Fitting windows and absorbers fitted in DOAS analysis. The representative wavelength for each target component is the cross-section-weighted mean wavelength over the fitting window.

Target component	Fitting window [nm]	Absorbers fitted	Representative wavelength [nm]
NO$_2$ (474 nm)	460–490	O$_3$, NO$_2$, H$_2$O, O$_4$, Ring	474
NO$_2$ (437 nm)	425–450	O$_3$, NO$_2$, H$_2$O, O$_4$, Ring	437
NO$_2$ (354 nm)	338–370	O$_3$, NO$_2$, HCHO, BrO, O$_4$, Ring	354

Table 2. Median values of retrieved NO$_2$ (volume mixing ratios (VMR) in the 0–1 km layer; ppbv) and estimated errors (ppbv) during cruise KY09-01. "Ocean" indicates NO$_2$ concentrations of less than 1 ppbv; "land" indicates latitudes higher than 33° N.

Component	VMR (ppbv)	Random error	Systematic error	Total error	# of data
NO$_2$ (476 nm) all	0.140	0.010	0.0176	0.020	735
NO$_2$ (476 nm) ocean	0.119	0.009	0.015	0.018	634
NO$_2$ (476 nm) land	8.858	0.179	0.951	1.050	88
NO$_2$ (437 nm) land	3.795	0.229	1.176	1.240	87
NO$_2$ (220 K) all	0.118	0.009	0.015	0.017	698
NO$_2$ (220 K) ocean	0.102	0.008	0.013	0.015	602
NO$_2$ (354 nm) all	0.204	0.023	0.032	0.043	607
NO$_2$ (354 nm) ocean	0.145	0.017	0.023	0.030	497
NO$_2$ (354 nm) land	9.673	0.259	1.483	1.713	93
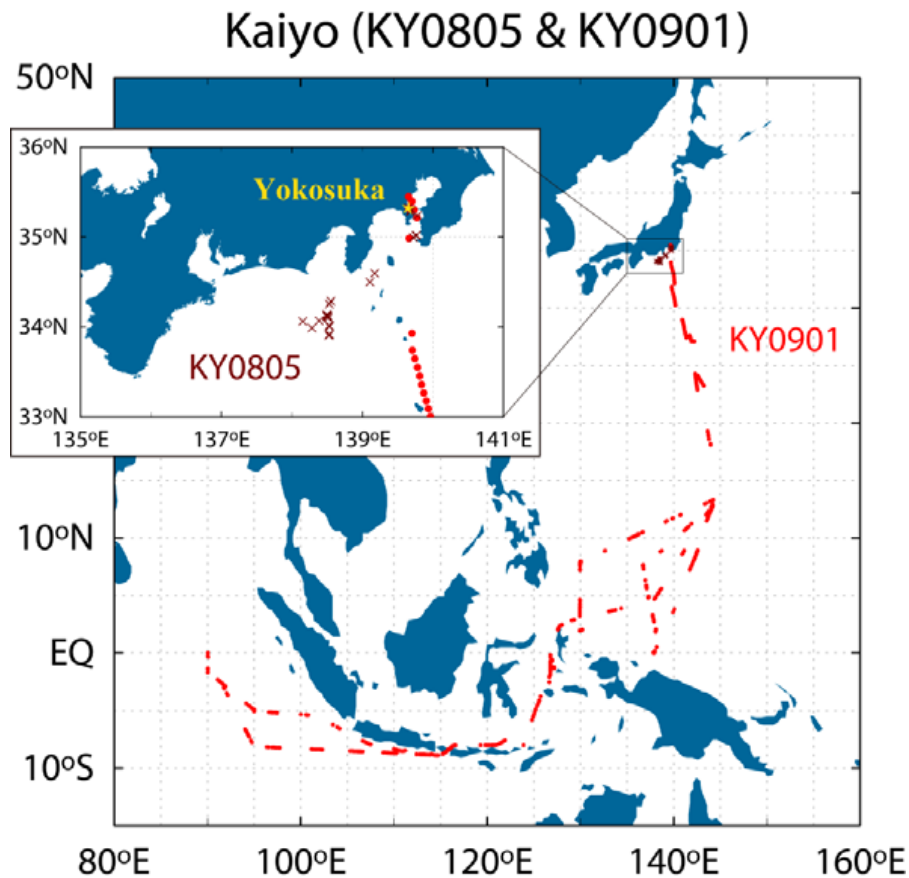
Fig. 1. Ship routes during the two ocean cruises by the Japanese R/V *Kaiyo* (KY0805 and KY0901).
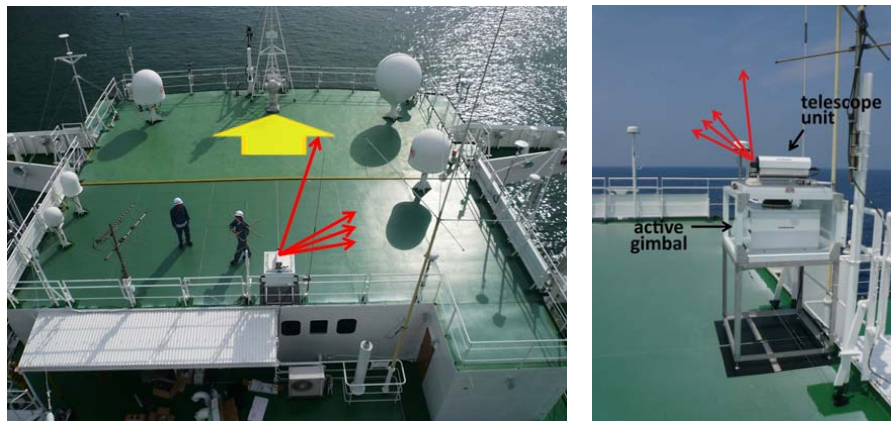
Fig. 2. Photographs of the outdoor unit of the MAX-DOAS instrument installed on the top deck of the R/V *Kaiyo*. The telescope unit was mounted on an active gimbal to ensure it was kept horizontal. The yellow arrow indicates the travelling direction of the ship. The line of sight of the instrument was toward starboard.
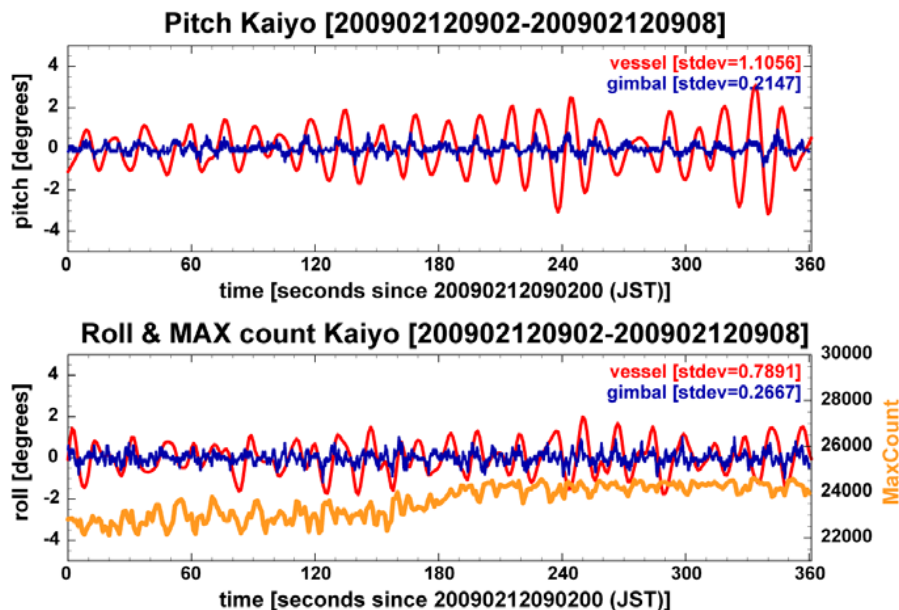
Fig. 3. Example of pitch (top) and roll (bottom) angles recorded for the vessel (red line) and the active gimbal (blue line). The yellow line indicates the maximum count of the spectrum. At approximately 180 s, the viewing elevation angle was changed from 3° to 5°.
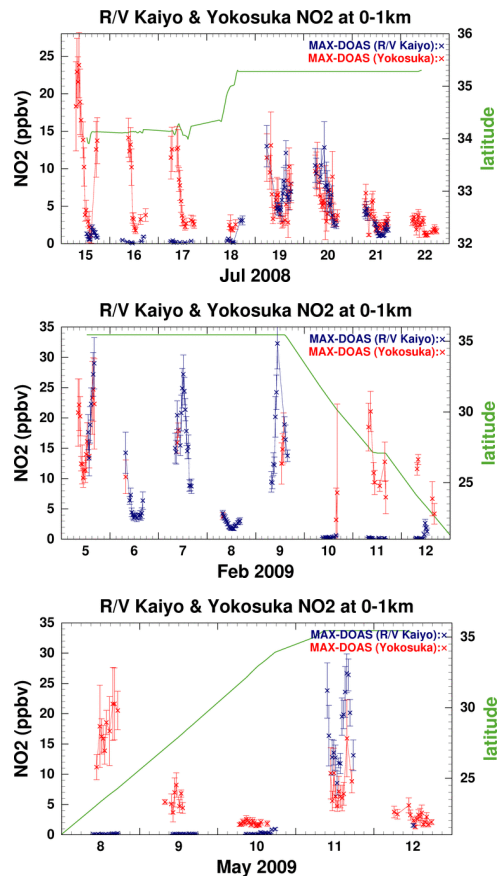
Fig. 4. NO$_2$ variations observed by MAX-DOAS on the R/V *Kaiyo* (blue) and at Yokosuka (red) for 0–1 km during the three observation periods, focusing on the Japan region. Error bars indicate the total error of NO$_2$ measurements. Also shown is the latitude of the vessel (green line).

Title Page

Abstract | Introduction

Conclusions | References

Tables | Figures

|◀ | ▶|

◀ | ▶

Back | Close

Full Screen / Esc

Printer-friendly Version

Interactive Discussion
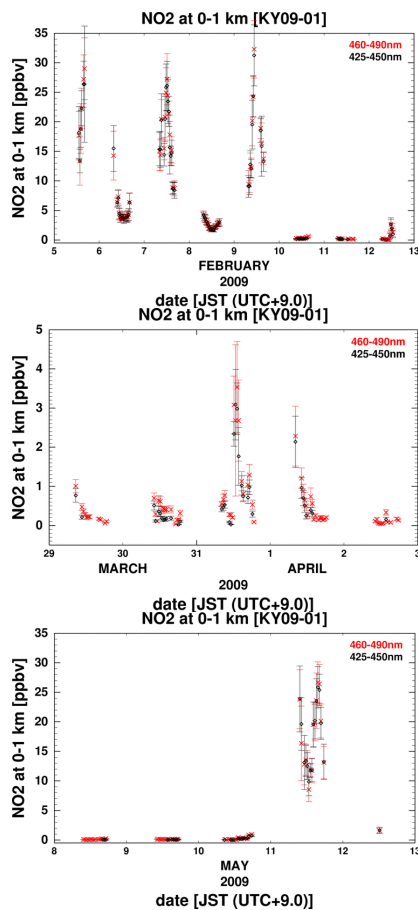
Fig. 5. As for Fig. 3, but for NO$_2$ concentrations measured on the R/V *Kaiyo* at 0–1 km for fitting windows of 460–490 nm (red) and 425–450 nm (black).
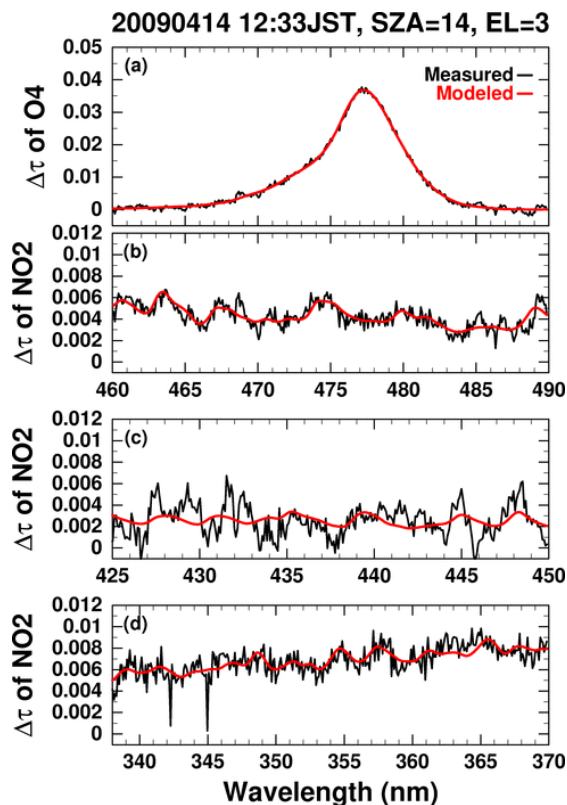
Fig. 6. Example of the result of nonlinear least squares spectral fitting for O_4 and NO_2 observed on 14 April 2009 on the R/V *Kaiyo* at 141.7° E, 11.1° N. For the NO_2 fittings, we used three fitting windows (460–490, 425–450, and 336–370 nm, as shown in **(b)**, **(c)**, and **(d)**, respectively). The red line shows the cross-section scaled to the spectrum (black) measured by DOAS. The spectra are plotted in terms of differential optical depth from the reference spectrum (elevation angle of 70°).
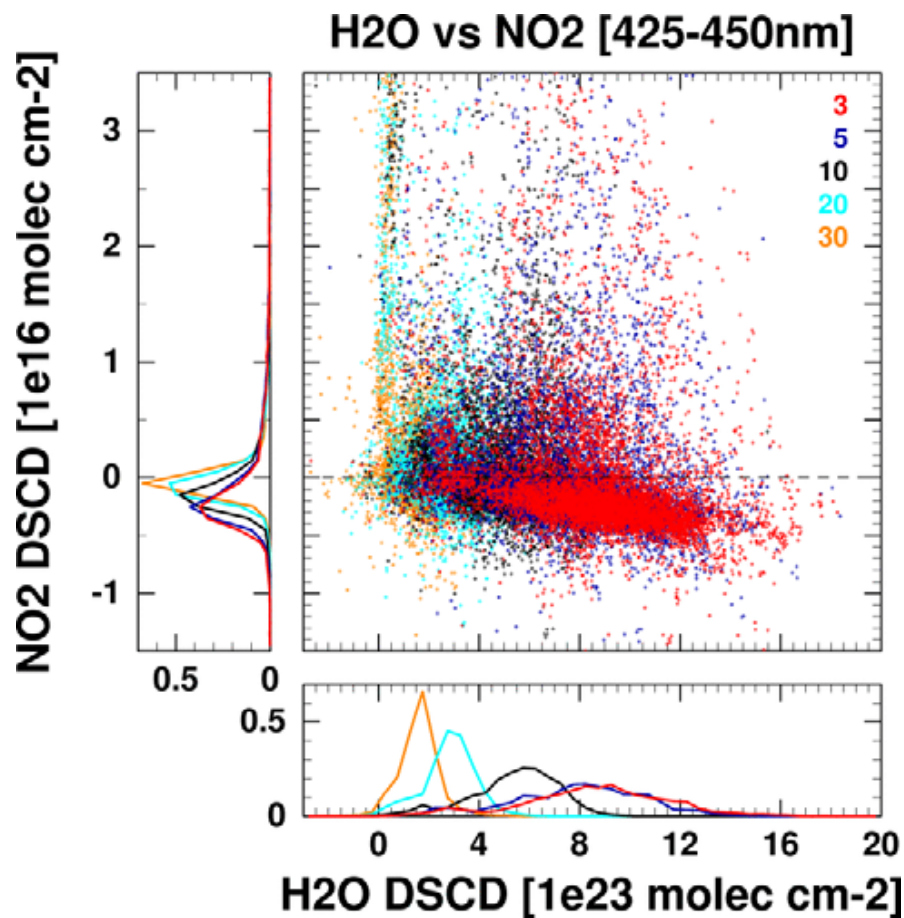
**Fig. 7.** Scatter plot of H_2O DSCD versus NO_2 DSCD for a fitting window of 425–450 nm at elevation angles of 3°, 5°, 10°, 20° and 30°.

Title Page

Abstract | Introduction

Conclusions | References

Tables | Figures

◄ | ►

◄ | ►

Back | Close

Full Screen / Esc

Printer-friendly Version

Interactive Discussion
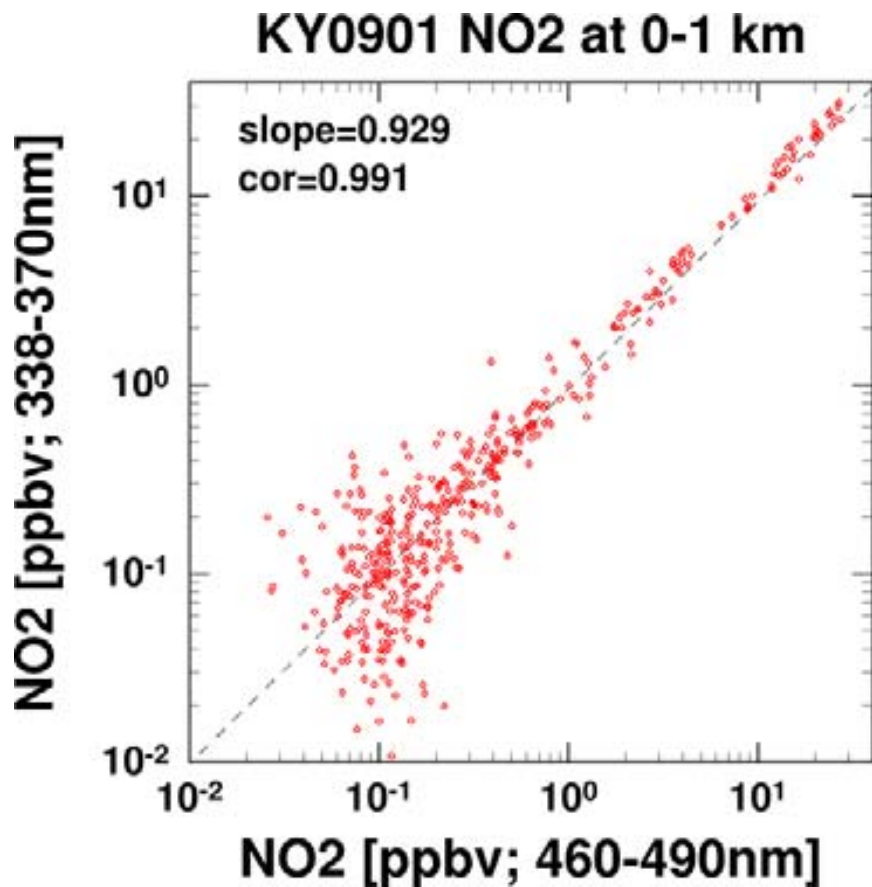
Fig. 8. Scatter plot of NO$_2$ concentrations for fitting windows of 460–490 and 338–370 nm during cruise KY0901.
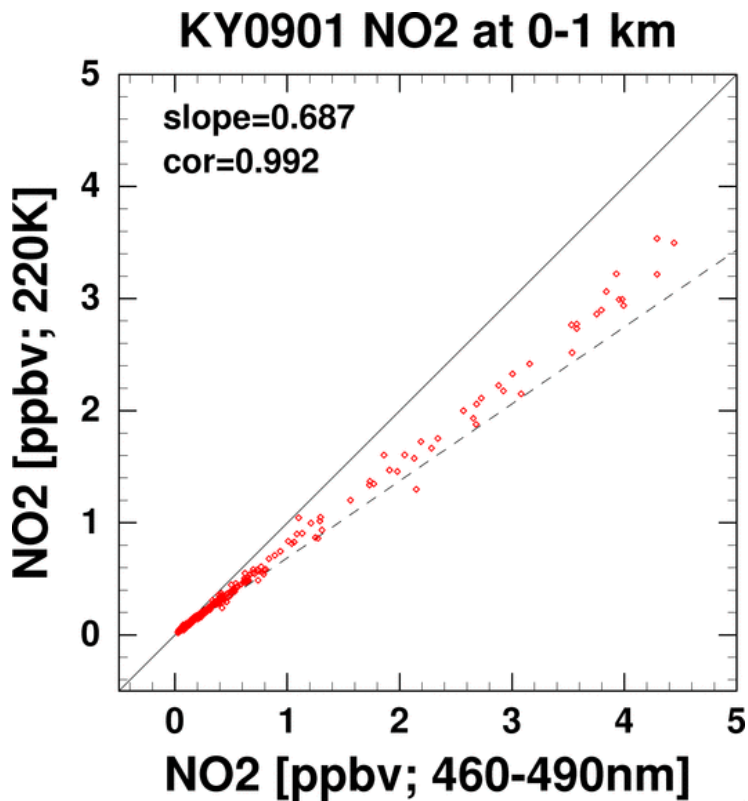
Fig. 9. Scatter plot of NO_2 concentrations for cross-sections at 294 and 220 K during cruise KY0901.

Title Page

Abstract | Introduction

Conclusions | References

Tables | Figures

◄ | ►I

◄ | ►

Back | Close

Full Screen / Esc

Printer-friendly Version

Interactive Discussion
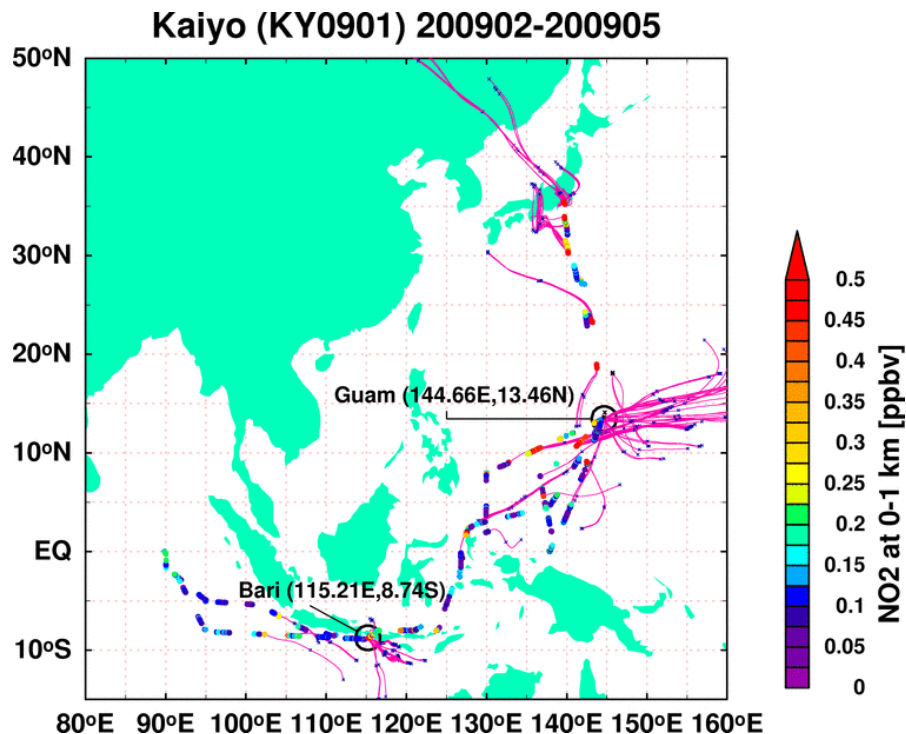
Fig. 10. NO$_2$ variations over the ocean for 0–1 km during the KY09-01 cruise. Pink lines show the 48-hour backward trajectory for NO$_2$ concentrations higher than 0.3 ppbv. The trajectory was calculated using meteorological analysis data from the Japan Meteorological Agency's Climate Data Assimilation System (JCDAS) reanalysis with a kinematic trajectory model.
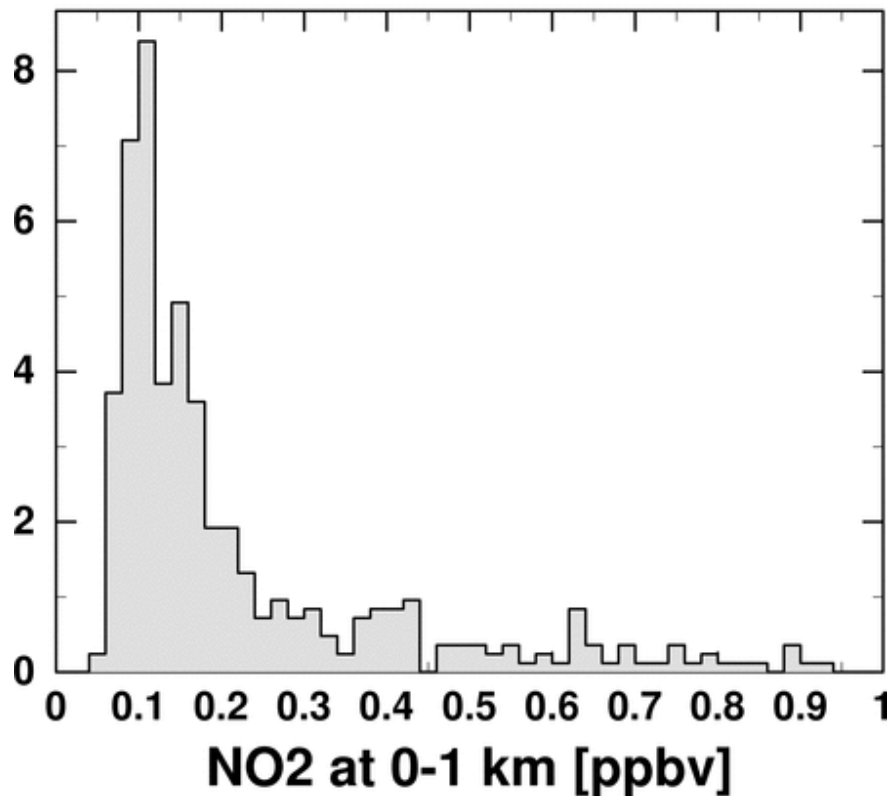
Fig. 11. Probability density function (PDF) of NO$_2$ concentrations at 0–1 km observed by MAX-DOAS for concentrations of <1 ppbv. The distribution has been normalized so that the integrated probability is equal to 1.

Title Page

Abstract | Introduction

Conclusions | References

Tables | Figures

◀ | ▶

◀ | ▶

Back | Close

Full Screen / Esc

Printer-friendly Version

Interactive Discussion